

1 Geochemical analysis unveils frictional melting process in a
2 subduction zone fault

3 **Tsuyoshi Ishikawa and Kohtaro Ujiie**

4

5 Supplemental Material

6

7 **METHOD**

8 **TABLES** (Tables DR1, DR2 and DR3)

9 **FIGURES** (Figures DR1, DR2, DR3 and DR4)

10

11

12

13

14

15

16

17

18

19

20

21

22

23 **METHOD**

24 **Sampling Method**

25 Dark veins and host rocks were sampled using a high-precision micro-mill Geomill326
26 (JAMSTEC, Izumo Web and Shimane University: see <http://geomill326.com/> for details) at the
27 Kochi Core Center (KCC), Japan. The Geomill326 is equipped with a micro-drill, a CMOS
28 camera and a movable sample stage, and allows automatic milling of a given micro-domain
29 through scanning of a drill bit by operation from a PC. A tungsten carbide bit or a single-crystal
30 diamond bit was used. In this study, the drill bit was placed on the rock surface at an angle of
31 about 60° and a rotation speed of 5,000 rpm, and repeatedly scanned within the focused area with
32 a depth of 20 µm and a width of 100 µm. Typically, 0.6 to 1.3 µg of samples were taken from the
33 pits with final depths of 300 to 600 µm. Surface images of the rock chip before and after
34 sampling are shown in Fig. DR1A and Fig. DR1B, respectively.

35 Because the host rock samples were taken from relatively small areas, it was not clear
36 whether they represented typical compositional variation in the host rock. Therefore, for
37 comparison, three additional samples were collected from a thin slice of the rear of the rock chip
38 as bulk rock samples (Fig. DR1C).

39

40 **Major and Trace Element and Sr Isotope Analyses**

41 The sample was weighed in a 7 mL PFA Teflon vial, and decomposed with 0.5 mL 38%
42 HF and 0.5 mL 68% HNO₃ at 120 °C. After dryness on the hot plate, 0.2 mL 70% HClO₄ and
43 subsequently 0.2 mL 6M-HNO₃ were added to the dried sample and repeatedly evaporated to
44 dryness at 180 °C. The sample was finally dissolved in 1 mL 3M HNO₃ (solution A), and the 0.2
45 mL aliquot was diluted with a mixed acid composed of 0.15M-HNO₃ and 0.015M-HF to give a

46 dilution factor of about 10,000 (solution B). Trace element concentrations in the sample solution
47 B were measured using an inductively plasma mass spectrometer (ICP-MS) Agilent 7700x at
48 KCC with the indium internal standard. For Sr isotope analysis, another aliquot containing
49 typically 200 ng Sr was taken from the rest of the sample solution A, and loaded onto a 0.2 mL
50 resin column (Eichrom Sr resin). After removal of other elements by adding 1 mL 6M-HNO₃ and
51 1 mL 3M-HNO₃, the Sr fraction was collected with 2 mL 0.05M- HNO₃. After dryness, about
52 100 ng Sr sample was loaded onto a W filament with Ta activator, and the Sr isotope ratio
53 (⁸⁷Sr/⁸⁶Sr) was measured using a thermal ionization mass spectrometer (TIMS) Thermo Finnigan
54 TRITON at KCC. Repeated analyses of NIST SRM 987 standard during this study gave an
55 average ⁸⁷Sr/⁸⁶Sr ratio of 0.710256. In the case where the sample solution A was still available,
56 the solution was diluted to give a dilution factor of 25,000 to 40,000, and measured for major
57 elements by ICP-MS. Major and trace element concentrations and ⁸⁷Sr/⁸⁶Sr ratio obtained for 0.9
58 mg of reference rock material JB-3 (Tables DR1 and DR2) were consistent with the reported
59 values (Geochemical reference samples database of Geological Survey of Japan:
60 <https://gbank.gsj.jp/geostandards/>).

61 In this study, we used CIPW normative composition of the samples for evaluating
62 relative abundances of plagioclase, quartz and illite-rich matrix. The CIPW norm is used
63 generally for igneous rocks, but useful for fault rocks, too, because it gives chemistry-based
64 quantitative estimates that are insensitive to comminution and secondary hydration and
65 recrystallization. However, SiO₂ content required for calculation of the CIPW norm is not
66 directly measurable by ICP-MS because of volatilization of SiF₄ during the sample
67 decomposition. Here a rough SiO₂ value was estimated by subtracting the sum of other major
68 oxides and 3.00 wt% H₂O from the total of 100.00 wt%. Then the CIPW norm of the sample

69 (Table DR1) was calculated assuming $\text{Fe}^{3+}/(\text{total Fe}) = 0.3$. Because the samples analyzed here
70 are all highly oversaturated with normative quartz (Q), uncertainty in the estimated SiO_2 value
71 only affect the calculated normative Q value, with the proportions of the rest of normative
72 minerals being unchanged. Although up to a few percent of uncertainty in the SiO_2 value (and
73 normative Q value) is expected due to possible variation in H_2O value for each sample, this does
74 not significantly affect the Q–Pl–Or relationship (Fig. 1A) and the normative-Or-based
75 discussion in this study.

76

77 **Evaluation of Element Contamination during Micro-milling**

78 The micro-sampling in this study was carried out using a tungsten carbide (WC) bit at the
79 beginning, and a diamond bit later. The use of WC is known to cause contamination of some
80 trace elements such as W, Co and Ta, while the contamination from diamond is likely to be
81 negligible. As two host rock samples, Ref-2 and Ref-4, were taken twice using different types of
82 bit (Ref-2T and Ref-4T by WC and Ref-2D and Ref-4D by diamond), the contamination from
83 WC is estimable by comparing these two sets of data. The samples taken with the WC bit show
84 clear enrichments of W, Co, V, Cr, Mo and Ta, which are not explainable by heterogeneity of the
85 sample in vertical direction (Fig. DR4A). Such WC-derived contamination is significant for
86 some of the quartz-plagioclase-rich host rocks with large hardness like Ref-2 and Ref-4, but
87 seems insignificant for other samples, except for W and Co. In fact, apart from Ref-2T and Ref-
88 4T, the values of Ta, V and Cr for micro-milled samples are consistent with those for bulk-rock
89 and mélange samples irrespective of the used bit type (Fig. DR4B, C), and the data form clear
90 trends consistent with $\text{Nb/Ta} = 13.5$ and $\text{V/Cr} = 1.69$ estimated for global subducting sediment
91 (GLOSS-II; Plank, 2014). Exceptionally high Cr concentration observed in Ref-6D (taken with

92 the diamond bit) possibly resulted from incorporation of Cr-rich micro-mineral phase. Thus the
93 contaminations of Ta, V and Cr (and possibly Mo) are likely to be minimal for most of the
94 samples. However, we decided not to include W, Co, V, Cr, Mo and Ta for any interpretation in
95 this study for clarity.

96

97 **Geochemical Modeling**

98 Concentration of an element in the host rock depends on concentrations of the element in
99 matrix (C_m) and plagioclase-quartz clasts (C_{pq}) and abundance ratio of these two components.
100 Letting a to be the weight fraction of the matrix ($0 \leq a \leq 1$), the element concentration in the host
101 rock (C_{host}) is given as

$$102 C_{host} = a C_m + (1 - a) C_{pq}. \quad (1)$$

103 Assuming that the weight fraction of the matrix (\approx melt) increases to b ($b > a$, $0 \leq b \leq 1$) but the
104 C_m and C_{pq} values remain constant during the frictional melting (i.e., selective, 100% melting of
105 the matrix), the element concentration in the resultant pseudotachylyte (C_{pt}) is given similarly:

$$106 C_{pt} = b C_m + (1 - b) C_{pq}. \quad (2)$$

107 Therefore, the enrichment factor of the element in the pseudotachylyte (F_E) can be defined as:

$$108 F_E = C_{pt} / C_{host} = [b C_m + (1 - b) C_{pq}] / [a C_m + (1 - a) C_{pq}]. \quad (3)$$

109 Then, let the relative abundances of the element in the matrix and clasts (p : $0 \leq p \leq 1$) and the
110 ratio of weight fraction of the matrix (\approx melt) in the pseudotachylyte to that in the initial host
111 rock (r) to be

$$112 p = C_{pq} / (C_{pq} + C_m), \quad (4)$$

$$113 r = b / a. \quad (5)$$

114 Combining equations (3), (4) and (5) gives:

115 $F_E = r + p(1 - r) / (a + p - 2pa) . \quad (6)$

116 In this modeling, it is essential to estimate the C_m and C_{pq} values for the elements
117 concerned. We estimated these values based on the correlation between the element
118 concentrations and the normative Or values of the host rocks, bulk rocks and dark veins (Fig.
119 DR3). The correlations observed in Fig. DR3 indicate the control by two-component mixing
120 between the Or-enriched matrix (and its melt) and the Or-depleted plagioclase-quartz clasts. We
121 assumed (1) the Or value of the matrix to be equal to that of illite (50.7) because the major
122 element composition of the pseudotachylite glass is close to that of illite (Fig. 2A), and (2) the
123 Zr concentration in the plagioclase-quartz clasts to be zero, which gives the Or value of 1.18. On
124 the basis of these Or values of two end-components, the C_m and C_{pq} values were calculated for
125 each element (Fig. DR3). The calculated F_E , C_m , C_{pq} and p values are listed in Table DR3.

126

127 **Reference**

128 Plank, T., 2014, The chemical composition of subducting sediments, *in* Holland, H., and
129 Turekian, K., eds., Treatise on geochemistry (second edition): Amsterdam, Elsevier, v.4,
130 4.17, p. 607–629.

TABLE DR1. MAJOR ELEMENT COMPOSITIONS AND CIPW NORM OF THE SAMPLES

Sample [*]	Dark veins					Host rocks								Bulk rocks							
	DkV1-1T	DkV1-2T	DkV1-3T	DkV2-2T	DkV3-1D	DkV3-2T	Ref-1D	Ref-2T	Ref-2D	Ref-3D	Ref-4T	Ref-4D	Ref-5D	Ref-6D	Bulk-1	Bulk-2	Bulk-3	Illite [†]	Laumontite [†]	JB-3	
(wt%)																					
SiO ₂ [§]	63.17	63.06	61.60	65.23	66.29	63.77	63.68	65.94	80.81	81.71	76.07	75.10	70.50	75.00	72.82	76.26	74.12	51.25	54.10	52.19	
TiO ₂	0.70	1.12	0.80	1.39	1.51	1.30	0.22	0.18	0.10	0.09	0.37	0.27	0.29	0.06	0.44	0.26	0.33	0.17	0.00	1.46	
Al ₂ O ₃	14.86	18.84	18.53	15.81	13.57	17.18	18.51	16.59	8.34	8.23	10.45	10.96	13.36	12.82	12.44	11.51	12.37	23.53	20.44	16.12	
Fe ₂ O ₃	7.49	4.66	5.40	5.63	6.54	5.35	4.08	3.50	2.01	1.60	3.63	3.73	5.53	1.92	4.49	2.73	3.27	2.39	1.70	11.19	
MnO	3.59	0.65	2.16	0.18	1.00	0.28	0.10	0.77	0.49	0.49	0.11	0.13	0.14	0.07	0.40	0.31	0.39	0.00	0.00	0.17	
MgO	1.00	1.69	1.35	1.35	1.28	1.51	0.90	0.76	0.47	0.34	0.79	0.80	1.08	0.35	0.77	0.53	0.59	3.32	0.45	5.05	
CaO	1.52	1.24	1.34	2.10	1.95	1.83	5.15	2.99	1.51	2.60	1.58	1.64	2.79	4.17	2.10	2.80	2.95	0.59	8.65	9.88	
Na ₂ O	0.47	0.58	0.58	1.17	1.62	1.62	1.91	5.00	2.55	1.32	2.77	2.95	1.33	1.67	1.49	1.30	1.52	0.05	2.60	2.67	
K ₂ O	4.04	5.00	5.09	3.93	3.03	4.00	2.43	1.22	0.68	0.60	1.17	1.37	1.89	0.95	1.98	1.24	1.40	7.61	0.55	0.76	
P ₂ O ₅	0.16	0.15	0.14	0.19	0.21	0.17	0.024	0.065	0.032	0.029	0.067	0.056	0.092	0.004	0.064	0.041	0.066	0.00	0.00	0.26	
CIPW norm (wt%)																					
Quartz	36.31	35.32	31.86	37.19	38.67	32.98	30.30	23.68	60.27	66.76	51.50	48.32	47.69	53.09	50.91	57.93	53.18	16.60	19.32		
Anorthite	6.79	5.30	5.98	9.57	8.58	8.20	26.31	14.87	7.49	13.10	7.63	7.99	13.68	21.33	10.36	14.08	14.67	3.27	48.08	0.40	
Diopside																					
Hypersthene	15.33	8.07	11.33	6.76	8.82	7.25	5.97	6.43	3.88	3.17	5.00	5.33	7.72	2.74	6.24	4.10	4.78	11.45	2.81		
Albite	4.15	5.08	5.08	10.24	14.22	14.22	16.75	43.66	22.25	11.59	24.20	25.81	11.59	14.55	13.03	11.34	13.28	0.51	24.88		
Orthoclase	24.76	30.61	31.14	24.05	18.56	24.47	14.83	7.45	4.14	3.66	7.15	8.33	11.58	5.79	12.11	7.56	8.57	50.70	3.66		
Apatite	0.37	0.37	0.32	0.44	0.51	0.42	0.05	0.16	0.07	0.07	0.16	0.14	0.23	0.16	0.09	0.16	0.16	0.09	0.16		
Ilmenite	1.39	2.20	1.58	2.73	2.98	2.54	0.42	0.34	0.21	0.17	0.74	0.53	0.57	0.11	0.85	0.51	0.65	0.36			
Corundum	7.57	10.95	10.30	6.47	4.75	7.53	3.52	1.85	0.79	0.76	1.99	1.86	4.44	1.52	4.32	3.14	3.25	15.92			
Magnetite	3.38	2.10	2.44	2.54	2.94	2.41	1.84	1.57	0.90	0.72	1.64	1.68	2.49	0.86	2.02	1.23	1.46	1.17	0.84		
Total	100.05	100.02	100.03	99.99	100.03	100.01	100.00	100.01	100.01	100.02	100.01	99.99	100.00	99.99	100.02	99.99	100.01	100.00	100.00		

Mugi samples with a final letter of "T" and "D" were sampled using a tungsten carbide bit and a diamond bit, respectively.

[†] Data from Deer et al. (1992)

[§] SiO₂ values for Mugi samples were calculated assuming H₂O = 3.00 wt% and Total = 100.00 wt%. The value for JB-3 was calculated assuming H₂O = 0.25 wt%.

TABLE DR2. TRACE ELEMENT AND Sr ISOTOPE COMPOSITIONS OF THE SAMPLES

Sample *	Dark veins							Host rocks								
	DkV1-1T	DkV1-2T	DkV1-3T	DkV1-4T	DkV2-1T	DkV2-2T	DkV3-1D	DkV3-2T	Ref-1D	Ref-2T	Ref-2D	Ref-3D	Ref-4T	Ref-4D	Ref-5D	Ref-6D
(ppm)																
Li	34.6	34.7	37.5	26.0	31.4	45.6	48.4	43.5	84.2	101	68.3	55.6	70.3	84.5	61.0	60.9
Be	4.39	4.00	4.34	5.18	4.31	3.85	2.89	2.83	1.04	1.31	0.730	0.553	1.07	1.17	1.40	0.548
K	35500	40400	42900	45000	32600	33400	25700	33100	17600	9590	5510	4840	8520	11100	16400	7760
Sc	15.7	23.4	20.3	22.1	18.5	24.8	21.5	23.7	5.17	3.62	2.34	1.84	6.17	6.16	6.04	2.06
Ti	4370	6430	4940	3740	5860	8360	7710	7760	1150	1030	604	493	2010	1620	1700	368
V †	116	154	134	153	128	160	121	159	40.1	131	15.4	18.3	74.6	39.9	50.3	13.6
Cr †	65.9	82.8	75.2	71.4	71.6	98.9	91.3	110	26.9	339	11.4	11.8	125	19.7	25.6	251
Mn	20000	4750	12400	7630	1640	1480	7480	2240	665	5860	3740	3720	722	966	1050	536
Co †	61.7	22.7	68.2	74.5	65.1	44.1	131	110	8.73	7260	16.5	31.4	2500	7.09	7.05	6.53
Ni	42.8	19.7	64.6	19.0	16.8	19.1	33.5	26.5	20.7	27.9	40.7	19.6	11.4	11.5	19.7	81.1
Zn	169	171	95	103	86.3	98.8	111	76.0	49.1	137	456	131	121	57.2	125	34.7
Ga	22.3	26.0	26.7	27.9	22.2	24.4	20.3	25.1	15.4	14.4	8.15	7.36	10.1	11.5	15.5	9.19
As	51.2	12.4	36.9	72.4	23.7	12.2	13.4	8.83	6.23	8.71	3.09	3.02	5.67	5.70	12.0	1.93
Rb	137	186	174	192	152	167	123	172	68.5	32.6	19.6	16.4	28.1	35.6	72.5	26.8
Sr	231	139	140	112	89.0	131	133	132	398	452	240	236	235	272	242	374
Y	32.1	38.7	31.3	30.2	38.0	55.9	53.5	52.0	9.45	9.17	5.84	4.20	13.9	13.6	12.1	2.75
Zr	211	254	218	247	185	347	261	256	42.6	45.7	26.7	20.4	88.5	69.9	69.3	11.9
Nb	14.3	21.2	16.4	11.9	19.1	28.5	25.0	24.3	4.23	4.43	2.30	1.61	8.69	5.95	5.40	1.28
Mo †	3.74	1.47	2.95	2.15	0.341	0.275	1.56	1.44	0.429	3.43	0.824	0.79	1.26	0.22	0.383	32.8
Cs	9.38	11.7	10.1	8.78	15.2	13.8	12.5	14.5	7.96	2.97	1.56	1.63	0.994	1.22	4.64	4.05
Ba	4550	864	1640	1190	455	487	913	392	575	705	420	398	411	544	339	434
La	73.4	28.8	33.2	32.4	38.1	59.9	53.2	27.0	14.9	24.3	17.5	8.76	27.8	25.4	8.15	4.50
Ce	73.0	65.5	87.1	62.6	90.1	129	103	63.5	29.9	37.3	26.7	26.7	45.0	41.4	13.7	9.02
Pr	12.4	6.75	6.91	6.36	10.7	15.7	13.9	10.0	3.88	4.41	3.11	1.70	5.29	4.84	2.52	0.917
Nd	43.0	26.3	25.5	24.0	42.3	59.8	56.5	43.5	15.4	15.9	11.0	6.04	18.9	17.3	10.7	3.46
Sm	6.83	6.04	5.13	4.53	8.49	12.5	12.3	11.1	3.03	2.58	1.74	1.04	3.33	3.18	2.53	0.637
Eu	2.69	2.43	2.02	1.71	2.13	3.07	3.25	2.88	0.616	0.807	0.509	0.348	0.965	0.877	0.684	0.234
Gd	6.46	6.55	5.27	4.79	7.87	11.3	11.4	10.6	2.37	2.13	1.36	0.874	2.89	2.64	2.37	0.542
Tb	0.891	1.01	0.826	0.732	1.17	1.72	1.70	1.64	0.316	0.311	0.183	0.131	0.439	0.399	0.363	0.083
Dy	5.54	6.97	5.43	5.06	7.73	11.0	10.6	10.5	1.97	1.72	1.16	0.805	2.78	2.63	2.25	0.552
Ho	1.18	1.47	1.17	1.12	1.49	2.16	2.11	2.05	0.374	0.350	0.231	0.164	0.542	0.528	0.467	0.100
Er	3.50	4.53	3.64	3.65	4.29	6.41	6.14	5.91	1.01	1.03	0.642	0.483	1.68	1.55	1.36	0.323
Tm	0.522	0.694	0.557	0.566	0.635	0.967	0.879	0.856	0.158	0.155	0.099	0.071	0.246	0.233	0.204	0.044
Yb	3.63	4.72	3.90	3.80	4.30	6.31	5.74	5.88	1.04	1.04	0.660	0.464	1.58	1.58	1.34	0.292
Lu	0.588	0.767	0.616	0.648	0.638	0.951	0.871	0.859	0.159	0.161	0.102	0.071	0.240	0.239	0.207	0.043
Hf	6.40	8.25	6.70	6.81	6.14	9.42	7.85	7.81	1.30	1.30	0.845	0.695	2.82	2.27	2.18	0.367
Ta †	1.03	1.50	1.26	1.00	1.33	2.02	1.87	1.77	0.267	1.74	0.172	0.128	1.17	0.314	0.322	0.079
W †	495	111	519	597	422	355	841	887	47.3	58700	125	244	21500	55.1	34.6	29.3
Tl	2.26	1.13	1.45	1.31	0.826	0.725	0.616	0.787	0.386	0.642	0.491	0.435	0.239	0.280	0.364	0.213
Pb	16.8	9.96	13.0	18.2	70.3	41.4	59.7	25.1	17.8	10.8	36.7	5.09	10.9	15.6	18.5	6.72
Bi	0.195	0.338	0.461	0.299	0.658	0.964	1.20	0.770	0.171	0.106	0.114	0.034	0.171	0.177	0.234	0.034
Th	21.4	26.5	22.0	21.9	20.3	31.8	26.4	27.1	6.47	4.61	2.85	4.46	7.55	7.08	5.24	1.06
U	3.47	4.85	4.11	4.24	3.80	6.18	5.21	5.11	0.977	0.966	0.685	0.624	1.68	1.53	1.31	0.281
⁸⁷ Sr/ ⁸⁶ Sr																0.709981

Mugi samples with a final letter of "T" and "D" were sampled using a tungsten carbide bit and a diamond bit, respectively.

† Elements not used for discussion because of possible contamination through sampling using a tungsten carbide bit.

TABLE DR2. (CONT.)

Sample *	Bulk rocks			Mélange matrices							(ppm)
	Bulk-1	Bulk-2	Bulk-3	1-5-1	1-5-2	1-5-3	2-2-1	2-2-2	2-2-3	JB-3	
Li	64.7	65.0	65.1	44.5	45.8	45.8	45.8	41.2	40.3	6.94	
Be	1.85	1.05	1.29	3.13	2.40	2.32	2.15	2.37	2.68	0.587	
K	16400	10300	11700	36200	29200	28000	25000	28500	31600	6230	
Sc	7.70	4.47	5.31	14.6	10.6	9.8	10.4	12.1	13.0	30.4	
Ti	2610	1580	1960	4690	3570	3350	3340	3800	4170	8670	
V †	59.5	33.4	37.9	109	82.0	79.1	80.5	88.0	94.2	384	
Cr †	25.3	14.1	17.5	51.8	36.4	35.0	35.5	41.6	45.1	84.0	
Mn	3110	2440	3010	1130	1040	888	802	883	920	1300	
Co †	6.00	6.74	5.15	11.3	6.52	3.80	2.47	3.59	6.38	33.3	
Ni	16.3	13.9	15.8	20.2	17.8	16.2	15.0	15.9	16.8	35.3	
Zn	73.3	58.0	66.2	67.9	56.2	48.5	50.1	54.2	55.6	103	
Ga	15.3	11.3	13.2	28.6	23.5	22.2	21.3	23.6	24.7	19.3	
As	12.0	6.72	8.72	12.1	5.51	5.21	7.02	11.5	13.9	1.92	
Rb	77.8	42.6	49.7	200	153	149	132	150	167	13.3	
Sr	223	266	273	127	166	171	213	194	161	395	
Y	21.4	13.8	17.9	29.5	22.2	20.2	21.1	22.7	24.4	22.2	
Zr	85.2	54.5	63.2	153	119	110	107	117	135	89.8	
Nb	6.61	5.01	5.86	15.2	11.7	11.0	10.9	11.8	12.9	1.88	
Mo †	0.67	0.557	0.650	0.971	0.419	0.282	0.469	0.952	0.966	1.01	
Cs	6.42	3.26	5.20	9.64	7.28	6.94	6.42	7.32	7.99	0.947	
Ba	718	545	714	512	504	483	409	446	475	225	
La	24.2	25.9	38.5	26.9	20.0	15.0	21.5	21.3	22.4	8.11	
Ce	42.4	55.0	77.9	70.5	52.0	40.7	53.6	55.7	58.7	19.6	
Pr	5.27	5.07	7.47	7.87	5.80	4.77	5.91	6.28	6.56	3.05	
Nd	20.0	17.8	25.6	30.0	22.1	18.4	22.0	24.0	25.7	14.9	
Sm	4.12	3.00	4.04	6.16	4.33	3.62	4.21	4.82	5.09	4.00	
Eu	1.25	0.890	1.22	1.45	1.07	0.937	0.989	1.09	1.20	1.26	
Gd	3.97	2.87	3.99	5.84	4.05	3.43	4.07	4.41	4.75	4.37	
Tb	0.574	0.368	0.477	0.877	0.615	0.494	0.577	0.681	0.695	0.685	
Dy	3.57	2.33	2.93	5.63	4.17	3.54	3.93	4.35	4.66	4.33	
Ho	0.734	0.449	0.561	1.16	0.864	0.745	0.781	0.880	0.941	0.917	
Er	2.10	1.33	1.71	3.51	2.58	2.42	2.48	2.68	2.89	2.58	
Tm	0.302	0.191	0.246	0.518	0.384	0.355	0.361	0.399	0.431	0.359	
Yb	2.05	1.29	1.57	3.47	2.68	2.38	2.44	2.66	2.88	2.35	
Lu	0.311	0.200	0.240	0.532	0.396	0.357	0.365	0.409	0.429	0.361	
Hf	2.53	1.63	1.93	5.04	3.49	3.25	3.26	3.97	3.84	2.73	
Ta †	0.353	0.362	0.372	1.20	0.908	0.876	0.866	0.927	1.01	0.113	
W †	0.134	0.506	0.232	1.46	1.16	1.09	1.13	1.27	1.33	1.36	
Tl	0.647	0.432	0.650	0.982	0.779	0.770	0.639	0.782	0.892	0.057	
Pb	19.3	16.4	15.7	30.6	25.6	22.2	18.5	23.1	29.4	4.90	
Bi	0.291	0.163	0.196	0.576	0.446	0.418	0.408	0.492	0.514	0.019	
Th	9.75	6.07	7.63	17.3	13.0	11.9	12.1	13.1	14.5	1.20	
U	1.82	1.17	1.46	3.41	2.51	2.30	2.41	2.60	2.88	0.443	
⁸⁷ Sr/ ⁸⁶ Sr	0.710790	0.710246	0.710363	0.714551	0.712800	0.712604	0.711929	0.712400	0.713152	0.703435	

TABLE DR3. PARAMETERS USED FOR MODELING

	Dark vein		Host rock		F_E	C_{pq}	C_m	p^*
	Average	1SD	Average	1SD				
(wt%)								
SiO ₂	63.86	1.67	76.53	4.15	0.83	80.06	47.33	0.628
Al ₂ O ₃	16.47	2.09	10.69	2.16	1.54	8.98	24.60	0.267
Fe ₂ O ₃	5.84	1.01	3.07	1.51	1.90	2.38	9.21	0.206
MgO	1.36	0.23	0.64	0.30	2.14	0.37	2.37	0.136
CaO	1.67	0.35	2.38	1.04	0.70	2.74	0.58	0.826
Na ₂ O	1.01	0.53	2.10	0.74	0.48	2.24	-0.33	1.000
(ppm)								
Li	37.7	7.6	66.8	10.2	0.56	73.6	9.76	0.883
Be	3.97	0.79	0.913	0.355	4.35	0.184	7.25	0.025
P	736	114	203	137	3.62	87.6	1310	0.063
K	36100	6330	9010	4240	4.00	1390	69700	0.020
Sc	21.3	3.0	4.10	2.22	5.18	-0.167	41.9	0.000
Ti	6150	1710	1130	721	5.43	150	12300	0.012
Mn	7200	6390	1790	1510	4.03	509	15020	0.033
Ni	30.2	16.5	30.7	26.9	0.99	24.1	42.1	0.364
Zn	114	36	154	153	0.74	137	85.0	0.618
Ga	24.4	2.6	10.3	2.9	2.37	6.75	41.9	0.139
As	28.9	22.9	5.24	3.67	5.51	0.539	45.4	0.012
Rb	163	24	33.2	20.4	4.91	0.384	320	0.001
Sr	138	41	267	54	0.52	294	17.7	0.943
Y	41.5	10.7	8.74	5.03	4.75	4.01	78.7	0.048
Zr	247	48	47.8	31.9	5.18	0.020	492	0.000
Nb	20.1	5.7	4.21	2.95	4.78	0.614	40.1	0.015
Cs	12.0	2.4	2.35	1.58	5.10	0.814	22.2	0.035
Ba	1310	1380	424	67	3.09	216	2670	0.075
La	43.3	16.9	15.4	9.7	2.82	15.0	70.9	0.175
Ce	84.2	23.2	27.1	14.4	3.11	26.3	139	0.159
Pr	10.3	3.5	3.06	1.73	3.38	2.75	17.4	0.136
Nd	40.1	13.8	11.2	6.1	3.57	9.50	68.2	0.122
Sm	8.37	3.24	2.07	1.12	4.03	1.43	15.0	0.087
Eu	2.52	0.54	0.603	0.291	4.19	0.310	4.82	0.060
Gd	8.03	2.71	1.78	0.99	4.51	1.10	14.8	0.069
Tb	1.21	0.41	0.266	0.152	4.55	0.131	2.27	0.055
Dy	7.86	2.52	1.69	0.97	4.63	0.740	14.8	0.048
Ho	1.59	0.45	0.339	0.196	4.70	0.128	3.03	0.040
Er	4.76	1.21	1.01	0.59	4.72	0.348	9.08	0.037
Tm	0.709	0.170	0.150	0.089	4.75	0.044	1.36	0.031
Yb	4.79	1.05	0.987	0.582	4.85	0.244	9.27	0.026
Lu	0.742	0.138	0.150	0.089	4.94	0.031	1.44	0.021
Hf	7.42	1.11	1.53	1.01	4.86	0.031	14.8	0.002
Tl	1.14	0.54	0.337	0.112	3.38	0.157	2.18	0.067
Pb	31.8	22.8	15.6	11.5	2.04	17.1	30.3	0.361
Bi	0.610	0.351	0.127	0.082	4.79	0.078	1.09	0.067
Th	24.7	3.9	4.71	2.48	5.24	0.389	49.0	0.008
U	4.62	0.88	1.02	0.56	4.54	0.213	8.99	0.023

* $p = C_{pq}/(C_{pq} + C_m)$. If $p_{\text{calc}} < 0$, p is regarded to be zero. If $p_{\text{calc}} > 1$, p is regarded to be 1.

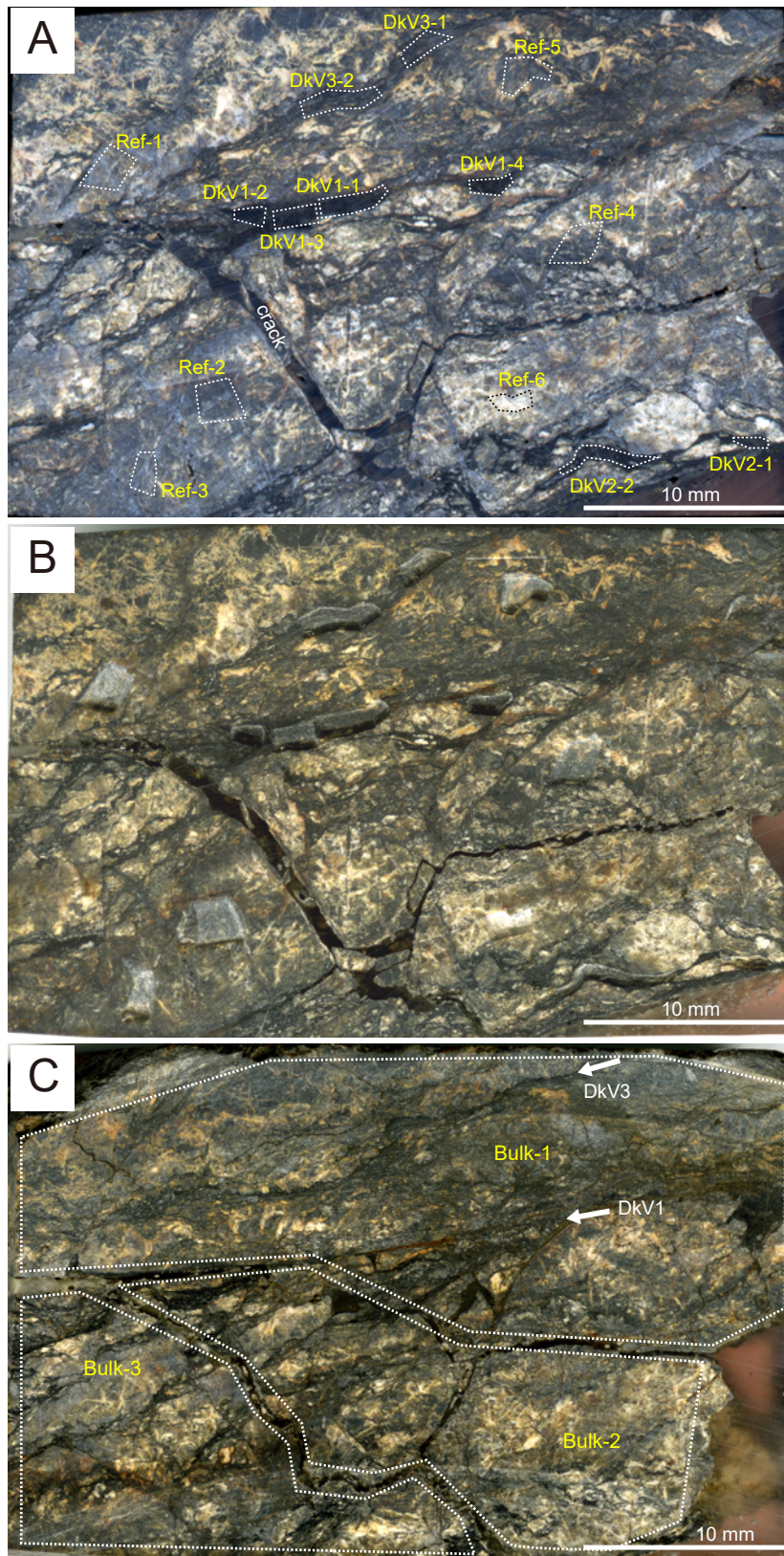


Figure DR1. Scanned surface images of the rock chip with sample points. A: Micro-sampled areas superimposed on the surface image before sampling. B: Surface image after sampling. Pits resulting from micro-milling can be seen. C: Surface image of the rear side of the rock chip (mirror-reversed image). Three bulk-rock samples were collected from a thin slice taken from this side.

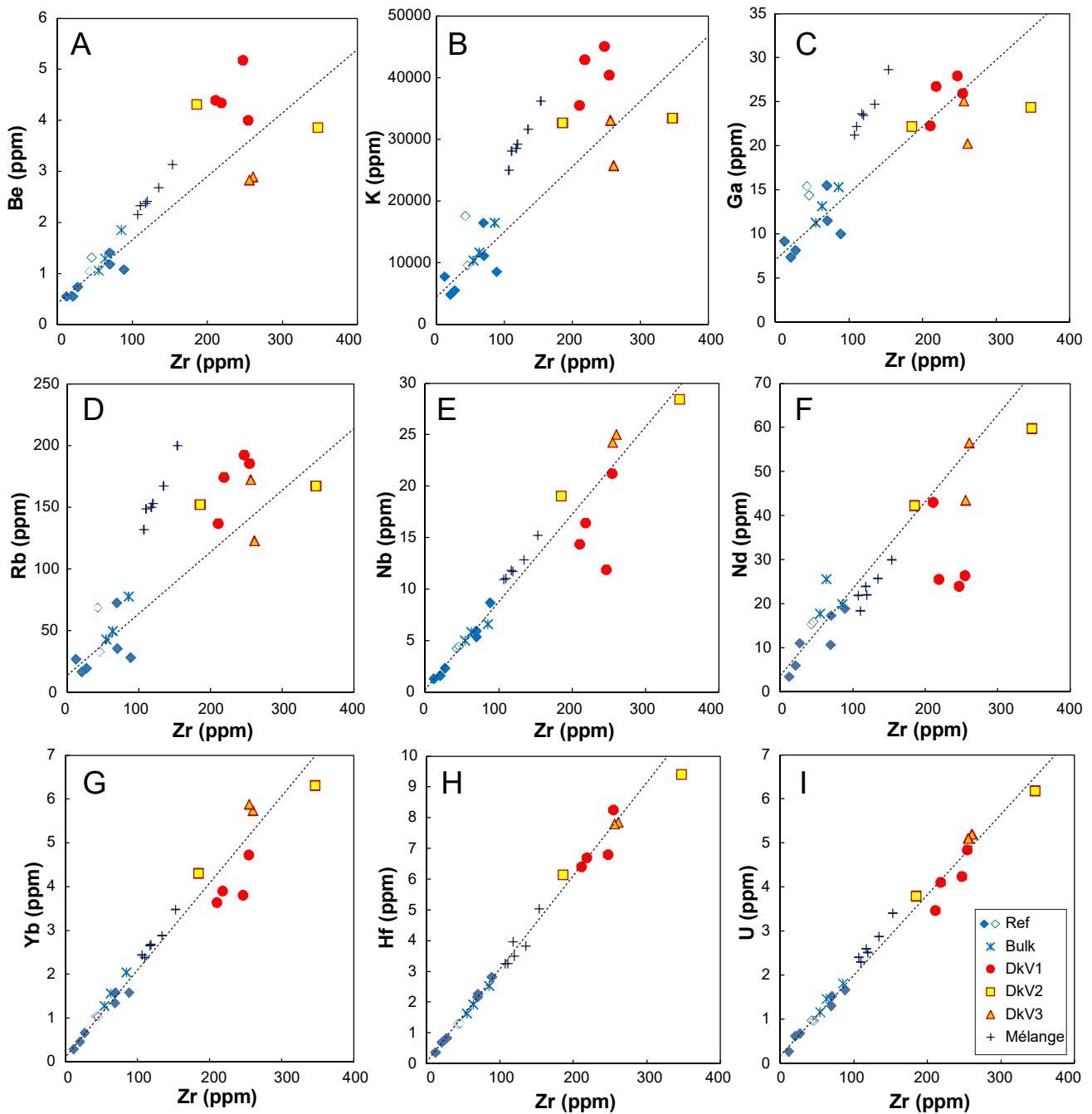


Figure DR2. Zr concentration versus trace element concentrations. Dotted lines indicate regression lines defined by compositions of host rocks (except for laumontite-rich samples shown by open diamonds) and bulk rocks. Note that K, Ga and Rb values of the mélange matrices deviate from the trends defined by host rocks, bulk rocks and dark veins (B, C and D), indicating that the mélange was not a source rock of the pseudotachylytes.

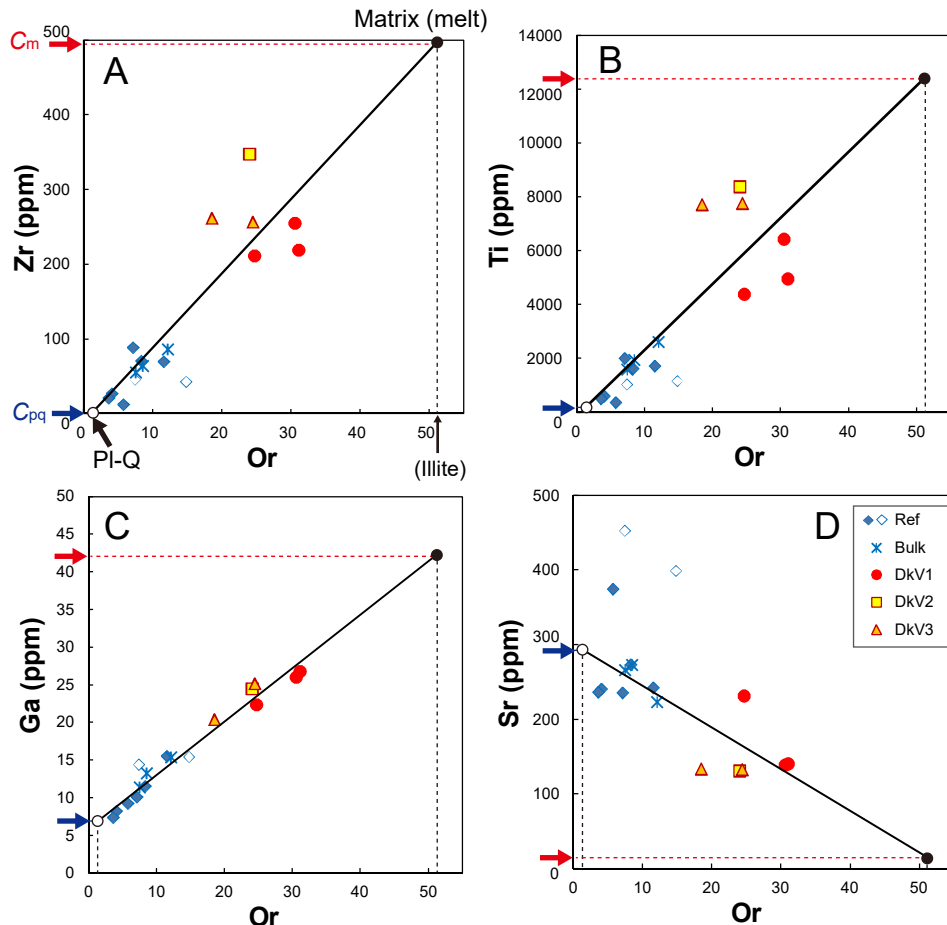


Figure DR3. Normative Or value versus trace element concentrations. Solid lines indicate regression lines defined by compositions of host rocks (except for laumontite-rich samples shown by open diamonds), bulk rocks and dark veins. Assuming Or values of the matrix and the plagioclase-quartz clasts to be 50.7 and 1.18, respectively, the C_m and C_{pq} values can be estimated (see Supplemental Material: Method).

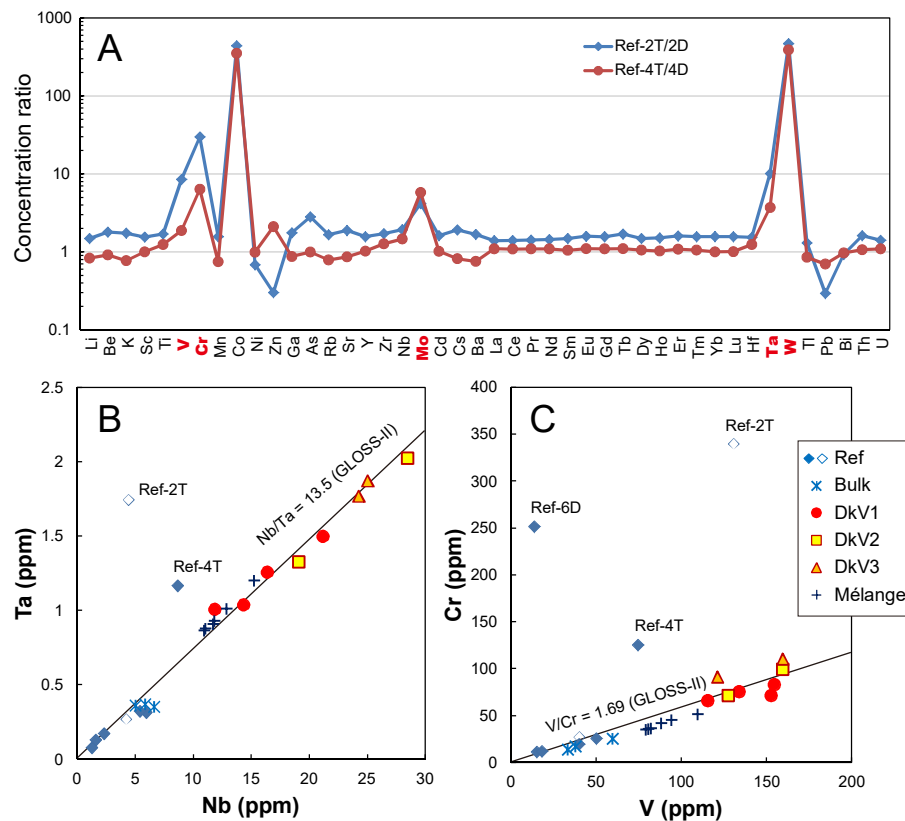


Figure DR4. Trace element contamination from tungsten carbide (WC) bit. A: Comparison of the trace element concentrations of the host rock samples taken by WC bit (Ref-2T and Ref-4T) with those taken by diamond bit (Ref-2D and Ref-4D). B: Nb concentration versus Ta concentration. C: V concentration versus Cr concentration. Solid lines in B and C represent Nb/Ta and V/Cr ratios of global subducting sediment (GLOSS-II). Contaminations of Ta, V and Cr from WC are insignificant except for Ref-2T and Ref-4T (see Supplemental Material: Method).